

Application of an advanced constitutive model in nonlinear dynamic analysis of tailings dam

A. R. Barrero & M. Taiebat
Department of Civil Engineering - University of British Columbia,
Vancouver, BC, Canada

A. Lizcano
SRK Consulting, Vancouver, BC, Canada



Challenges from North to South
Des défis du Nord au Sud

ABSTRACT

Tailings are residual material produced during the process of extraction of minerals from mined ores. Saturated tailings are usually retained in the impoundments by means of raised embankments (tailings dams). These are constructed in stages over the life of the impoundment with compacted natural soil, tailings materials and/or waste rock. Due to the usually huge dimensions of the impoundments, the great heights of the embankments and the site conditions like saturated loose granular foundation materials and high PGA, tailings dams represent a high-risk construction for the environment in case of a dam failure. In general, detailed numerical studies are conducted for seismic analyses of high-risk tailings dams during the design phase. However most of the analyses are performed using very simplistic stress-strain models such as Mohr-Coulomb model even for loose sand layers. For the present study the SANISAND constitutive model was implemented in the finite difference code FLAC as a dynamic-link library. Then the liquefiable sand layer of a tailings dam under a seismic motion was analyzed using this more representative model. A number of representative results of the dynamic analysis including contours of shear strain and time history of the excess of pore pressure ratio for are presented and discussed. Results of the analysis suggest that at least for the analyzed motion the safety of the dam is not compromised.

RÉSUMÉ

Les résidus miniers sont des matériaux résiduels produits lors du processus d'extraction d'une exploitation minière. Les résidus saturés sont habituellement retenus dans des bassins par des digues surélevées (barrage de résidus). Ceux-ci sont construits par étapes, sur la durée de vie de la retenue avec de la terre compactée naturelle, des matériaux de résidus/stériles et des roches. À cause des dimensions énormes des retenues d'eau, de la hauteur des digues et des conditions du site, telles que les fondations en matériaux granulaire saturés et la forte accélération maximale du sol (PGA en anglais), les barrages en résidus représentent un risque élevé pour l'environnement en cas de rupture. En général, des études chiffrées sont réalisées concernant les analyses sismiques des barrages en résidus à haut risque durant la phase de conception. Cependant, la plupart des analyses réalisées utilisent un modèle très simpliste de contrainte-déformation, tels que le modèle de Mohr-Coulomb même pour des couches de sable meuble. Dans l'étude actuelle, SANISAND a été analysé pour une activité sismique utilisant la méthode des différences finies avec FLAC. Ensuite, la couche de sable liquéfiable d'un barrage de résidus avec un mouvement sismique a été analysée en utilisant ce modèle plus représentatif. Un certain nombre de résultats représentatifs de l'analyse dynamique, notamment les contours de déformation de cisaillement et l'évolution dans le temps de l'excès de taux de compression de pore, sont présentés et discutés. Les résultats de l'analyse indiquent qu'au moins pour le mouvement analysé, la sécurité du barrage n'est pas compromise.

1 INTRODUCTION

Tailings are waste products resulting from mining operations. These are pumped in a slurry form to an impoundment and usually retained by embankments (tailings dams). Embankments are raised in multiple stages by the upstream, downstream, or center-line construction methods. These embankments and the tailings dam foundation may be found comprising by different soil types with different layer orientations and thicknesses, and zones varying from fine to coarse materials that vary in density, under a wide range of confining pressures and drainage conditions. These layers experience various loading conditions during the construction stages and then may be subjected to seismic loading during the life of the tailings dam.

The safety of tailings dams must be guaranteed well beyond the period of the mining activity according to

governmental requirements. Safety in this context is related to the long-term performance of the structure and its stability under static and dynamic loadings. Liquefaction assessments of tailings dam and foundation layers should be included as part of the dam performance and stability and to guarantee the dam safety.

Under the previously outlined complex conditions and related to material types, layering, relative densities, confining pressures, drainage conditions, and loading types, representative deformation analysis of the tailings dam is a challenging task. It requires extensive engineering effort to decide what aspects of soil behavior should be prioritized in the analyses. The task can be significantly reduced if the constitutive and numerical model of the dam account for many of the essential conditions described before. The use of representative models help reducing the epistemic uncertainty in the analyses. Of course constitutive models can still over or

under predict results depending on the calibration of the model parameters. Also their application should not go beyond modeling the mechanisms that the formulation of the model is designed for.

In this paper, the Simple ANIsotropic SAND (SANISAND) constitutive model described in Manzari and Dafalias (2004) was implemented and added as a dynamic linked library (DLL) for the two-dimensional non-linear finite difference code Fast Lagrangian Analysis of Continua or FLAC (Itasca Consulting Group 2012). This model was used to illustrate how the engineering effort can be reduced if an advanced constitutive model is used. For this purpose, a liquefaction assessment is performed in numerical modeling of a dam section comprising of a loose sand layer. The numerical model was built following construction procedures and it was subjected to an earthquake input motion to determine the occurrence of the liquefaction phenomena and the overall stability and performance of the dam.

2 CONSTITUTIVE MODEL

SANISAND is the name used for a family of Simple ANIsotropic SAND constitutive models within the frameworks of critical state soil mechanics and bounding surface plasticity (Manzari and Dafalias 1997, Dafalias and Manzari 2004, Dafalias *et al.* 2004, Taiebat and Dafalias 2008, Li and Dafalias 2012). In the present paper the focus is on seismic wave propagation and liquefaction. To involve fewer model parameters and for simplicity, the version of the SANISAND model with fabric change effects (Dafalias and Manzari 2004) has been considered as the constitutive model for the soil. The inherent anisotropy (Dafalias *et al.* 2004), the plastic strains under constant-stress ratios (Taiebat and Dafalias 2008), and the anisotropic critical state (Li and Dafalias 2012) have not been accounted for in the present work.

A brief overview of the basic formulation of SANISAND used in this paper will be presented in triaxial space. The model is fully compatible with a multiaxial stress-space generalization. Both stresses and strain quantities are assumed to be positive in compression. All the stress components in this paper must be consider as effective stress. Triaxial stress and strain components are defined as deviatoric stress $q = (\sigma_1 - \sigma_3)$, mean pressure $p = (1/3)(\sigma_1 + 2\sigma_3)$, deviatoric strain $\varepsilon_q = (2/3)(\varepsilon_1 - \varepsilon_3)$, and volumetric strain $\varepsilon_v = (\varepsilon_1 + 2\varepsilon_3)$. The stress ratio is represented by $\eta = q/p$.

2.1 Elastic and plastic strains

The nonlinear elastic response of the SANISAND model is assumed to be hypoelastic. The strain increment is decomposed to elastic and plastic parts, denoted by the superscript e and p , each one having deviatoric and volumetric parts, denoted by subscripts q and v :

$$d\varepsilon_q^e = \frac{dq}{3G}, \quad d\varepsilon_v^e = \frac{dp}{K} \quad [1]$$

$$d\varepsilon_q^p = \frac{d\eta}{H}, \quad d\varepsilon_v^p = d|d\varepsilon_q^p| \quad [2]$$

where K and G are the hypoelastic bulk and shear modulus, H is the plastic hardening modulus associated with the increment of stress ratio $d\eta$, and d is the dilatancy coefficient. Variables H and d will be defined later. The incremental bulk and shear modulus are defined according to Richart *et al.* (1970) and Li and Dafalias (2000):

$$G = G_0 p_{at} \frac{(2.97 - e)^2}{1 + e} \left(\frac{p}{p_{at}}\right)^{1/2}, \quad K = \frac{2(1 + \nu)}{3(1 - 2\nu)} G \quad [3]$$

where G_0 is a dimensionless material constant, ν is the Poisson's ratio, e is the void ratio, and p_{at} is the atmospheric pressure used for normalization.

2.2 Critical state

SANISAND is formulated within the critical state soil mechanics framework. The location of the critical state line that defines the critical void ratio e_c is given by the power relation after Li and Wang (1998):

$$e_c = e_{c0} - \lambda_c \left(\frac{p_c}{P_{at}}\right)^\xi \quad [4]$$

where e_{c0} is the void ratio at $p_c=0$, λ_c and ξ are dimensionless material constants. The model uses the concept of the state parameter ψ proposed by Been and Jefferies (1985) to define the distance between the current void ratio and the critical void ratio:

$$\psi = e - e_c \quad [5]$$

2.3 Yield surface

The yield surface can be imagined as a tiny wedge in the p - q space and a cone in the multiaxial space. The yield function is expressed by:

$$f = |\eta - \alpha| - m = 0 \quad [6]$$

where the m is a material constant representing the opening of the yield surface and α is the deviatoric back stress ratio representing the orientation of the yield surface.

2.4 Dilatancy, bounding and critical surfaces

The model uses three concentric and homologous surfaces: the dilatancy, bounding and critical surface. These are considered in the π -plane. The dilatancy surface is defined by the slope of M^d . This surface enables the model to reproduce contractive volumetric soil response if $\eta < M^d$, and dilative volumetric soil response for $\eta > M^d$. The evolution of the dilatant surface is defined by the state parameter ψ as:

$$M^d = M \exp(n^d \psi) \quad [7]$$

where M and n^d are positive material constants. The bounding surface is defined by the slope of M^b . This surface enables the model to reproduce softening if $\eta > M^b$, this will result in a peak shear stress in the stress-strain curve. The evolution of the bounding surface is again defined by the state parameter ψ as:

$$M^b = M \exp(-n^b \psi) \quad [8]$$

where n^b is positive material constant. As the sample reaches the critical state, and the distance between the critical void ratio and current void ratio is close to 0, hence the lines representing M^d and M^b converge and collapse with the critical surface line M .

2.5 Plastic flow

The used SANISAND model includes a non-associative flow rule allowing realistic evaluations of plastic strain increments with equation [2]. In this equation H controls the increment of the plastic deviatoric strain as a function of distance between M^b and η :

$$H = h(M^b - \eta) \quad [9]$$

where h is a function of current state variables p and e . The dilatancy coefficient d in equation [2] is expressed through:

$$d = A_d(M^d - \eta) \quad [10]$$

where A_d is a function of the fabric dilatancy.

2.6 Numerical implementation

In the present paper FLAC (Itasca Consulting Group 2012) is used as the main platform to explore a boundary value problem. FLAC uses explicit time-integration scheme, fully coupled solid-fluid interaction and large strain deformation, and is well suited to solve dynamic stability problems. The constitutive model was implemented as a user-defined material for FLAC and compiled as DLL to enable new users to call the model. To verify details of the implementation several single element tests were carried out and compare with an implemented stand-alone constitutive driver in *MATLAB*, as explained also in Taiebat *et al.* (2011). Moreover several drained and undrained monotonic and cyclic triaxial laboratory test data on Toyoura sand, after Verdugo and Ishihara (1996) and Pradhan *et al.* (1989), were reproduced with the implemented model. The validation results are not presented here to keep the simplicity of the paper. Future publication will describe details of numerical implementation of the model and its efficiency tests.

3 DESCRIPTION OF THE PROBLEM

3.1 Geometry and layering of tailings dam section

Figure 1 shows the section of the tailings dam chosen for the analysis. This section is a typical geometry of a tailings dam built by the center-line method. The section in Figure 1 includes the foundation soil stratigraphy, the materials of the embankment, the tailings material, and the water level.

The foundation soil comprises of three main layers. The upper deposit is assumed to be a 10 m thick alluvial layer of sandy gravel to gravelly sand with a density varying from compact to dense. The bottom layer is assumed to be a glacio-fluvial deposit with variable thickness overlying weathered bedrock. Its thickness varies from 25 m at the right to 7 m at the left boundary of the section shown in Figure 1, and its density varies from compact to very dense. Embedded in between these two layers is a 3 m thick potentially liquefiable sand layer with relative density of around 50%. The base weathered bedrock is assumed to have a relatively low shear wave velocity.

The body of the dam is mainly composed by sand and gravel. It includes a 14 m high starter dam of waste. The density along the dam body is supposed to varies from dense to very dense, but for modeling purposes a dense density is assigned.

The tailings material typically are found to have a wide range of density from very loose to compact, in this study it was assumed to be a compact material. The height of tailings dam in the analyzed section is around 36 m.

3.2 Material properties

General mechanical properties of the various layers shown in Figure 1 are summarized in Table 1. The mechanical behavior under monotonic and dynamic loads of the potentially liquefiable sand layer was modeled with SANISAND. The constitutive parameters for SANISAND in the potentially liquefiable sand layer were taken after the model validation by Taiebat *et al.* (2010), and are presented in Table 2. The values for the material constant M was calculated from the friction angle provided in Table 1. The behavior of the other layers was modeled using Mohr-Coulomb model with hysteretic damping to approximately match the modulus reduction and damping curves of Seed and Idriss (1970).

Table 1. Mechanical material parameters for different layers in Figure 1.

Layer	ϕ^* (°)	c (kPa)	V_s (m/s)	ν	γ (kN/m ³)
Bedrock	40	0	760	0.31	20
Glacio-Fluvial	40	0	380	0.26	15.6
Liq. Sand	28	0	262	0.33	14.4
Alluvial	35	0	353	0.26	16.0
Waste rock	34 [8]	2	343	0.306	15.8
Tailings	33	0	265	0.27	19.9
Filter Material	34	0	330	0.33	15.8
Rock fill	34	0	330	0.33	15.8

* Dilatation angle is assumed to be 0 unless stated otherwise in [].

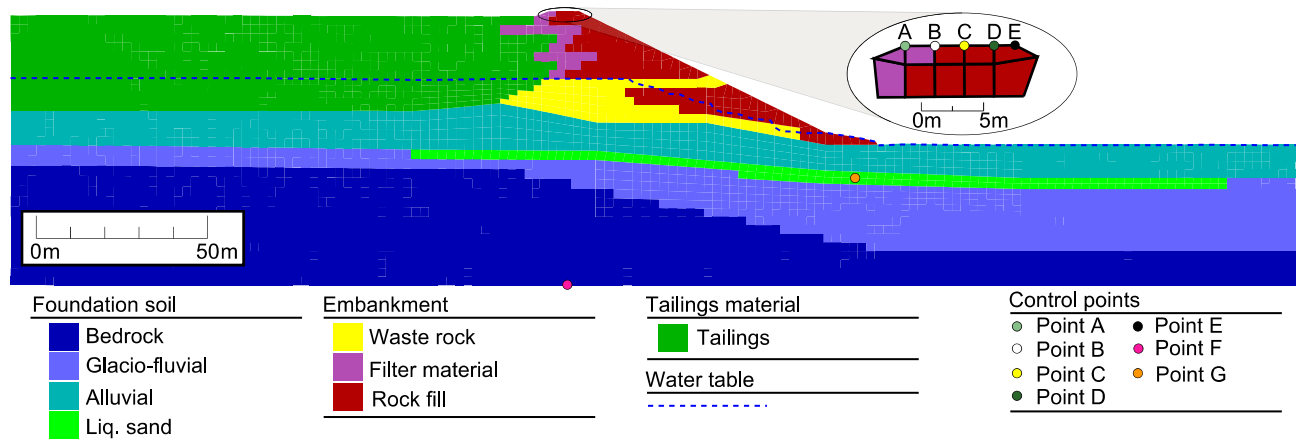


Figure 1. Stratigraphy of the tailings dam section and soil foundation.

Table 2. Material parameter used in SANISAND constitutive model for the potentially liquefiable sand layer.

Parameter	Symbol	Value	Parameter	Symbol	Value
Elasticity	G_0	125	Dilatancy	n^d	125
	ν	0.05		A_0	0.05
Critical state	M	1.11	Kinematic	n^b	1.11
	c	0.712		Hardening	h_0
	e_{c0}	0.934		c_n	0.934
	λ	0.019	Fabric dilatancy	Z_{max}	0.019
ξ	0.7	c_z		0.7	

3.3 Earthquake motion

The earthquake motion was chosen from the PEER (2015) ground motion database. The motion was selected after linear scaling to a typical Uniform Hazard Spectral (UHS) for northern British Columbia at the base of the model (soil class C – average shear wave velocity 360-760 m/s). A moment magnitude range of $M_w = 6.5-7.5$ and a distance of about 10–30 km was considered in the selection criteria. The motion was then spectrally matched to the target UHS in the period range of 0.02–2s using the computer program SeismoMatch (Seismosoft 2009a) as shown in Figure 2. Additionally, the motion was baseline corrected and frequency cut at 6Hz with the computer program SeismoSignal (Seismosoft 2009b). A summary of the selected earthquake motion including its horizontal peak ground acceleration (PGA) and moment magnitude M_w is provided in Table 3.

Table 3. Information about the scaled ground motion.

Motion	Year	Station	M_w	PGA (g)
Darfield, New Zealand	2010	OXZ	7.0	0.26

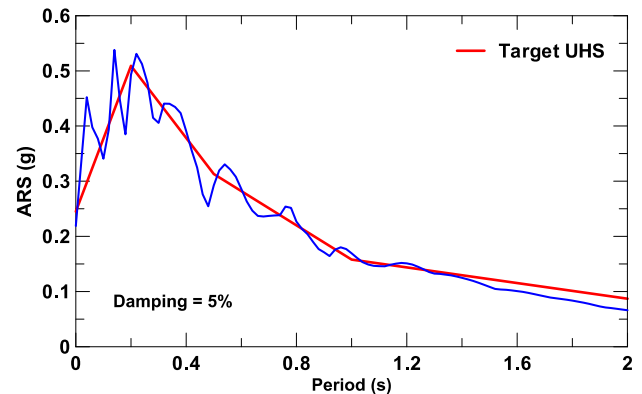


Figure 2. Acceleration response spectrum of the motion spectrally matched to the UHS of the site.

4 NUMERICAL MODEL OF THE DAM

4.1 General

Figure 3 shows the FLAC discretization used for the continuum model along with the boundary conditions for the static analysis. Control points A-E in Figure 1 show the locations where data was recorded during the analysis and evaluated in the results section of the paper. These include five points along the crest of the dam, one point at the base of the model and one point in the middle of the potentially liquefiable sand layer. The numerical model was constructed in layers and brought to equilibrium under self-weight in 4 consecutive stages.

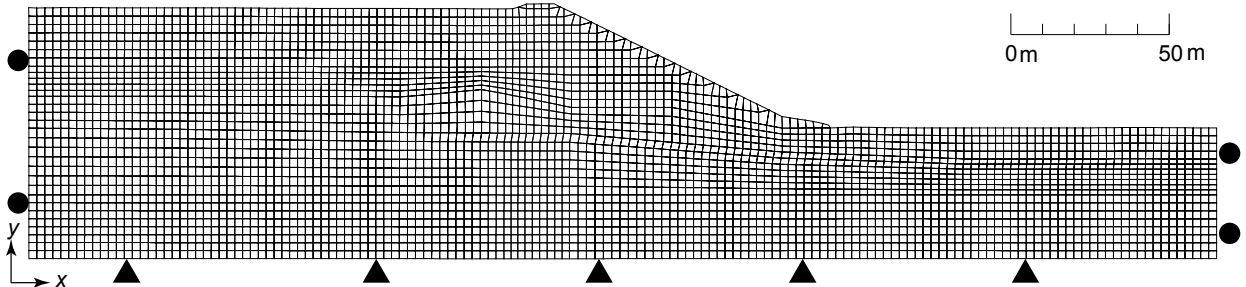


Figure 3. Model discretization and boundary conditions for the self-weight stage (the latter is changed for the seismic stage).

4.2 Sequence of analysis

The numerical analysis accounts for both mechanical response of solids and hydro-mechanical response of pore fluid. First a pure mechanic calculation was conducted to establish the in-situ stresses. The water bulk modulus (K_w) was set zero to avoid any excess of pore pressure. During this phase the numerical model was built with a layer-by-layer scheme. Typical roller boundary conditions are applied to the side boundaries and fixed boundary condition was applied to the base. All material groups were assumed to be Mohr-Coulomb for this phase. The system was brought to equilibrium under increments of self-weight load.

In the second stage, the mechanical calculation is turned off and the fluid is turned on to initialize the hydrostatic pore water pressure. The phreatic surface was quickly developed after the saturation was initialized in each element. The saturation was set to 1 and 0 for zones below and above the water table, respectively.

In the next stage, the SANISAND model was assigned to the potentially liquefiable sand layer and it was brought to equilibrium. The velocity and displacements in the grid points were then set to 0 so that the dynamic stage would start from a non-deformed grid.

The final stage was the dynamic excitation. For this stage the fluid was set off and the water bulk modulus was given a realistic value of 2 GPa. The side boundaries were replaced with free-field boundaries, to allow the motion to travel upward along the side boundaries without distortion as to those with lateral infinite boundaries. The base was set to quite boundaries to prevent reflect the waves back into the system. The seismic motion was applied to an elastic layer at the base as a shear stress history. At this stage the dynamic simulation includes a full fluid and mechanical interaction.

The zones set with the SANISAND model were assigned with a low Rayleigh damping (0.5%) at a central frequency of 1Hz to reduce the high frequency noises. Other zones were assigned a higher Rayleigh damping (2%) at a central frequency of 2Hz. For the Mohr-Coulomb layers additional FLAC hysteric default damping was added to better capture the modulus reduction and damping within the elastic region of this model.

5 RESULTS

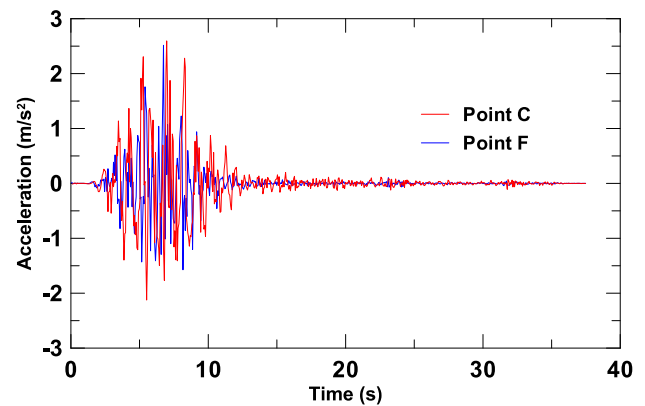


Figure 4. Time history of horizontal component of acceleration.

Figure 4 shows time histories of the horizontal acceleration at the crest of the dam (Point C in Figure 1) and at the bottom of the model (Point F in Figure 1). In this Figure, some amplification can be observed as the motion is propagates through the soil layers.

Contour plot of the maximum shear strain at the end of the earthquake motion is shown in Figure 5. Shear strains are developed mainly near the crest of the dam and in the toe mainly in the potentially liquefiable sand layer but also extending to the surface. The region with the maximum shear strain in the sand deposit occurs near point G of Figure 1 with shear strains around 2.0-2.5%. The displacement vectors at the end of earthquake loading are presented in Figure 6. These vectors illustrate the residual deformation pattern. The maximum displacement of 0.43m is located at the top of the downstream face.

Changes of vertical effective stresses σ'_v caused by the ground motion can be monitored by the excess of pore water pressure ratio (R_u) defined as

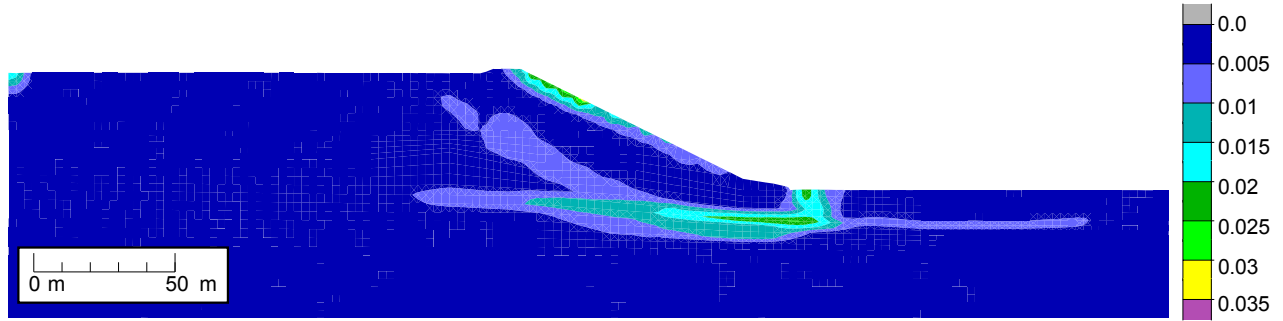


Figure 5. Contour plot of maximum shear strains at the end of earthquake excitation.

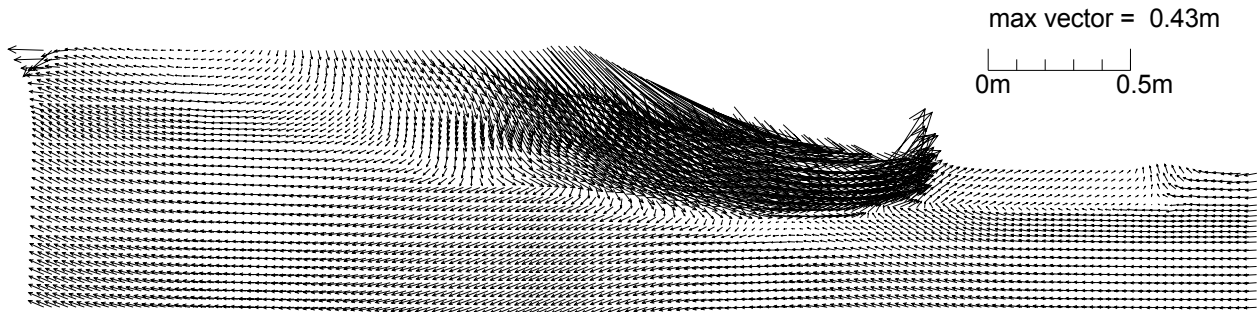


Figure 6. Displacement vectors at the end of earthquake excitation.

$$R_u = \frac{u_e}{(\sigma'_v)_{in}} = 1 - \frac{\sigma'_v}{(\sigma'_v)_{in}} \quad [11]$$

where u_e is the excess pore water pressure and $(\sigma'_v)_{in}$ is the effective vertical stress before the shaking. Note that u_e can be defined as $u_e = p_w - (p_w)_{in} = (\sigma'_v)_{in} - \sigma'_v$, where p and $(p_w)_{in}$ are the current and initial pore pressure, respectively. Note that an extreme value of $R_u = 1$ corresponds to the full loss of effective stress ($\sigma'_v = 0$). Figure 5 shows time history of the excess of pore water pressure ratio at control point G in the potentially liquefiable sand layer. The numerical results show that the R_u developed during the major part of shaking (first 10 seconds) does not exceed 0.6. The corresponding shear strain at this point is around 2.5% (not shown here)

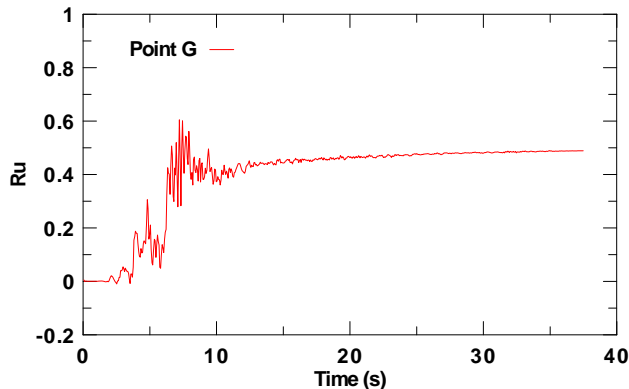


Figure 7. Time history of the excess pore pressure ratio at control point G.

A major performance criteria for checking the safety of the dam is the resulting settlement at the crest due to seismic excitation. The elevation of the crest of the dam before and after the shaking, and also the elevation of tailings material are presented in Figure 8. The results presented in this figure suggest that the crest settlement (in average is 20cm) after the shaking does not compromise the safety of the dam as the dam crest remains above the elevation of the tailings. This is a guarantee that an overtopping of the tailings material will not occur after the motion.

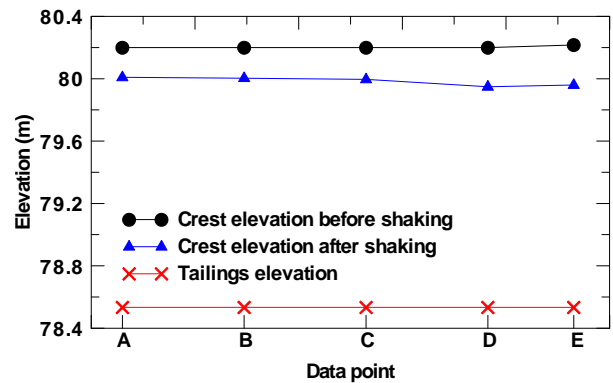


Figure 8. Elevations of the dam crest before and after the shaking for the points in Figure 1 (elevation of tailings material shown for reference).

6 CONCLUSIONS

The Manzari and Dafalias (2004) SANISAND model was implemented and added to FLAC as a user-defined material using the DLL. The model is able to capture granular soils in wide ranges of confining pressures and densities using the same set of parameters. In particular it can capture cyclic behavior that could trigger liquefaction. Such advance models can serve as effective tool to properly capture various aspects of stress-strain response and reasonably reduce the engineering effort in evaluation and modeling of response in complex soil systems. In this paper a typical tailings dam section was subjected to an earthquake motion to perform a seismic analysis and assess response of a potentially liquefiable sand layer in the foundation deposits. Results of analysis show that although there is a loss of effective stress the motion does not triggers the flow liquefaction phenomena. The results also show acceptable performance of the dam after shaking in terms of the settlement measures at the crest level.

ACKNOWLEDGEMENTS

Authors would like to thank Dr. Katerina Ziotopoulou for discussion on constitutive model implementation, and Mr. Boris Kolev for the help with discretization of the tailings dam. Support to conduct this study is provided by MITACS Canada and SRK Consulting.

REFERENCES

- Been, K., and Jefferies, M.G. 1985. A state parameter for sands. *Geotechnique*, 35(2), 99-112.
- Dafalias, Y.F., and Manzari, M.T. 2004. Simple plasticity sand model accounting for fabric change effects, *Journal of Engineering Mechanics*, 36(1): 65 - 78.
- Dafalias, Y.F., Papadimitriou, A.G., and Li, X.S. 2004. Sand plasticity model accounting for inherent fabric anisotropy, *Journal of Engineering Mechanics*, 130(11): 1319-1333.
- Itasca. 2012. FLAC: Fast Lagrangian Analysis of Continua. Version 7.0. Itasca Consulting Group, Inc., Minneapolis, Minn.
- Li, X.S., and Dafalias, Y.F. 2000. Dilatancy for cohesionless soils. *Geotechnique*, 50(4), 449-460.
- Li, X.S., and Dafalias, Y.F. 2012. Anisotropic critical state theory: role of fabric, *Journal of Engineering Mechanics*, 138(3): 263-275.
- Li, X.S., and Wang, Y. 1998. Linear representation of steady-state line for sand. *J. Geotech. Geoenviron. Eng.*, 124(12), 1215-1217.
- Manzari, M.T., and Dafalias, Y.F. 1997. A two-surface critical plasticity model for sand. *Geotechnique*, 47(2), 255-272.
- Pradhan T.B., Tatsuoka F, Sato Y. 1989. Experimental stress-dilatancy relations of sand subjected to cyclic loading. *Soils and Foundations*, 29(1): 45-64.
- PEER. 2015. Pacific Earthquake Engineering Research Center strong motion database. [Accessed on 7 May 2015.]
- Richart, F.E., Jr., Hall, J.R., and Woods, R.D. 1970. Vibration of soils and foundations. *International series in theoretical and applied mechanics*, Prentice-Hall, Englewood Cliffs, N.J.
- Seed, H. B., and I.M. Idriss. Soil Moduli and Damping Factors for Dynamic Response Analysis. Earthquake Engineering. Research Center, University of California, Berkeley, Report No. UCB/EERC-70/10, p. 48 (1970).
- Seismosoft. 2009a. SeismoMatch. Version 1.0.3.
- Seismosoft. 2009b. SeismoSignal. Version 4.1.2.
- Taiebat, M., and Dafalias, Y.F. 2008 SANISAND: simple anisotropic sand plasticity model, *International Journal of Numerical and Analytical Methods in Geomechanics*, 32(8): 915-948.
- Taiebat, M., Jeremic, B., Dafalias, Y.F., Kaynia, A.M., and Cheng, Z. 2010. Propagation of seismic waves through liquefied soils. *Soil Dynamics and Earthquake Engineering*, 30(4): 236-257.
- Taiebat, M., Kaynia, A.M., and Dafalias, Y.F. 2011. Application of an anisotropic constitutive model for structured clay to seismic slope stability. *Journal of Geotechnical and Geoenvironmental Engineering*, 137(5): 492-504.
- Verdugo, R. 2009. Seismic performance based-design of large earth and tailing dams, *Performance-Based Design in Earthquake Geotechnical Engineering*, ICPBD Conference, Tsukuba, Japan: 41-60.
- Verdugo, R., and Ishihara, K. 1996. The steady state of sandy soils. *Soils Found.*, 36(20), 81-92.